Jacek KANIEWSKI[1]
Zbigniew FEDYCZAK[1]

MODELLING AND ANALYSIS OF THREE-PHASE HYBRID TRANSFORMER USING MATRIX-REACTANCE CHOPPER

This paper deals with the modelling and analysis of a new solution for a three-phase AC transformer with electromagnetic and electric coupling (hybrid coupling). The electromagnetic coupling is realized by means of the conventional three-phase transformer (TR) with two secondary windings in each phase. The electrical coupling is realized by means of a three-phase matrix-reactance chopper (MRC) with Ćuk topology. This paper presents an operational description, a modelling and a theoretical analysis of the properties of the proposed solution. The steady-state analysis is based on the averaged state-space method, D-Q transformation and four terminal descriptions, and is verified by the simulation investigations. Dynamics analysis is based on Laplace's transformation and small signal model, and is verified by the simulation investigations.

1 INTRODUCTION

The defining quality parameters of electric energy are well known, and described in [1]. The dynamic states in alternating current (AC) power transmitting system, such as fault switching effects, dynamic load changes, or atmospheric discharge on the consumer side generate undesirable effects such as voltage sags, interruptions and swells. Poor quality electrical energy has a negative effect on sensitive devices. In computers, transceiver devices, medical systems, production line, electric motors supplied from frequency converters, erratic supply parameters cause failure or defective devices [2]–[5]. In the case of industrial customers, voltage perturbation in supply voltage may cause very large financial damage [6].

Secondary supply sources, such as constant-voltage regulators or voltage sag compensators, attenuate the unwanted effects of supply [7]–[15]. The conventional solution for AC voltage regulators are based on a classic electric transformer with mechanical or thyristor tap changer. These devices have disadvantages, which are described in [16]. The application of AC-AC converters using pulse width modulation (PWM) control strategy to construct secondary supply sources eliminates disadvantages of conventional

[1] Faculty of Electrical Engineering, Computer Science and Telecommunications, University of Zielona Gora, Zielona Góra, 65-246 Poland tel.+48 68 328 2538, J.Kaniewski@iee.uz.zgora.pl, Z.Fedyczak@iee.uz.zgora.pl

AC voltage regulators. The devices described in [7]–[9], [11], [13], [14] and [15] guarantee fast changing output voltages and satisfactory dynamic properties. The fundamental disadvantage of these solutions is lack of galvanic separation between source and load. This property is very important from the point of view of an AC distribution system. The conception of a single-phase new generation distribution transformer is presented in [13], where a conventional transformer works together with a unipolar matrix converter. A more thorough analysis of such a solution is presented in [17] and is developed by using matrix-reactance choppers in [18] and [19].

The presented solution has two couplings (hybrid coupling), an electromagnetic one realized by means of conventional transformer and an electric one realized by means of a matrix-reactance chopper, and is therefore called a hybrid transformer (HT). The three-phase HT using matrix converter is described in [20]. This paper develops the conception of a three-phase HT by using a matrix-reactance chopper with Ćuk topology. In this paper, there is an operational description, modelling and a theoretical analysis of the static and dynamic properties of the proposed solution.

2 DESCRIPTION OF THE PROPOSED SOLUTION

The schematic diagram of the proposed solution of hybrid transformer is shown in Fig. 1.

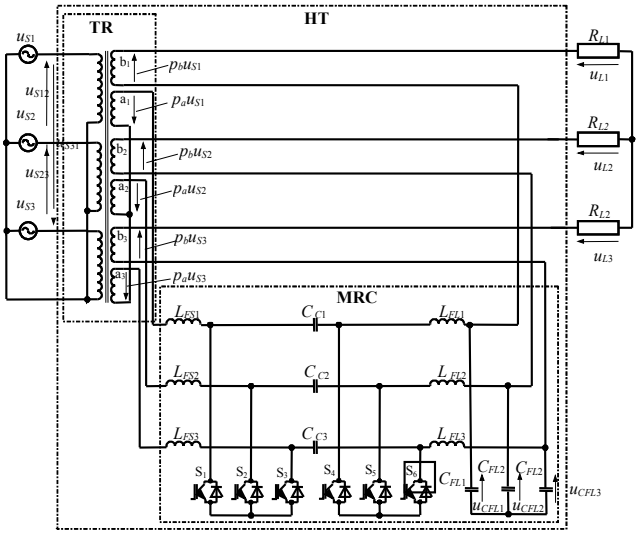

Fig.1. Three-phase hybrid transformer using MRC with Ćuk topology

As is visible in Fig. 1 the circuit of the considered HT contains two main units. The first one is a three-phase conventional transformer (TR), the second one is a three phase matrix-reactance chopper (MRC) with Ćuk topology [21]. The transformer has two secondary windings in each phase. Primary windings are Y-connection. The main secondary windings of TR (a_1, a_2, a_3) also have Y-configuration, and they are connected with MRC. Secondary phase windings (b_1, b_2, b_3) are connected in series with phase output

connectors of the MRC respectively. Secondary voltages of the windings a_1, a_2 and a_3, have opposite phase in relation to secondary voltages of the windings b_1, b_2 and b_3. Output voltages of the MRC (u_{CFL1}, u_{CFL2}, u_{CFL3}) are shifted in phase about π in relation to voltages $p_b u_{S1}$, $p_b u_{S2}$, and $p_b u_{S3}$. Therefore output voltages of the presented HT are an algebraic sum of the output voltages of MRC (u_{CFL1}, u_{CFL2}, u_{CFL3}), and secondary voltages of TR ($p_a u_{S1}$, $p_a u_{S2}$, $p_a u_{S3}$). Transformer voltage ratios of the windings *a* and *b* are p_a=4/3 and p_b=2/3 respectively. These values are the same as in [13], [17], [18], [19] and [20]. Exemplary idealized voltage time waveforms illustrating operation of the presented HT are shown in Fig. 2.

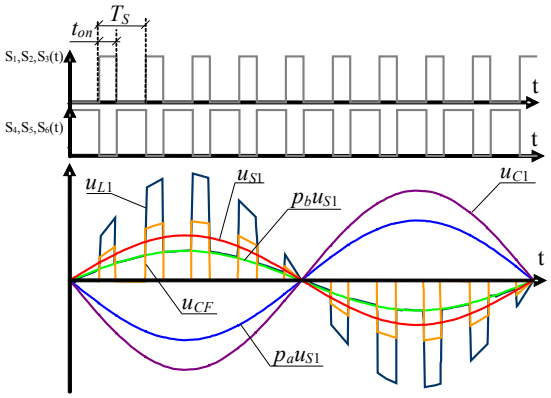

Fig.2. Control signal and idealized voltage time waveforms in circuit of HT, D < 0.5, f = 500 Hz

The duty factor of the control signal of the MRC switches is expressed as:

$$D = \frac{t_{on}}{T_S} \tag{1}$$

The output voltages of the MRC (u_{CFL}) with Ćuk topology and output voltages of the considered HT (u_L) shown in complex form by means of an idealized equation are described by (2) and (3) respectively.

$$\underline{U}_{CFL} \cong p_a \underline{U}_S \frac{D}{1-D}, \tag{2}$$

$$\underline{U}_L \cong p_a \underline{U}_S \frac{D}{1-D} + p_b \underline{U}_S \cong \underline{U}_{CFL} + p_b \underline{U}_S . \tag{3}$$

According to (2) the idealized transmittance of the MRC with Ćuk topology can be written as:

$$\left| \underline{H}_U^{MRC} \right| \cong \left| \frac{\underline{U}_{CFL}}{p_a \underline{U}_S} \right| \cong \frac{D}{1-D} . \tag{4}$$

According to (3) the idealized voltage transmittance of the presented HT can be described as:

$$\left|\underline{H}_U^{HT}\right| \cong \left|\frac{\underline{U}_L}{\underline{U}_S}\right| \cong p_a \frac{D}{1-D} + p_b . \tag{5}$$

The graphical interpretation of (3) and (4) is shown in Fig.3.

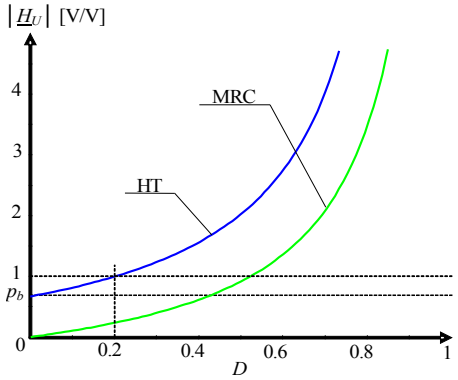

Fig.3. Idealized characteristics of the MRC and HT voltage transmittances as a function D

As is visible from Fig. 3, the output voltage of the HT is less than the source voltage for $0 \le D \le 0.2$. For $0.2 < D < 1$, the output voltage of the presented HT is greater than the supply voltage.

3 THEORETICAL ANALYSIS

3.1 Averaged model of HT

An equivalent schematic diagram of the presented HT (Fig. 1) with ideal switches is shown in Fig. 4.

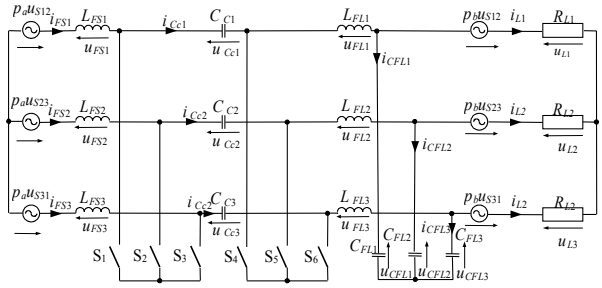

Fig.4. Equivalent schematic diagram of the HT with ideal switches

Theoretical analysis is based on the averaged state-space method [21], [22], and d-q transformation method [23]. In the considered circuit, there are two operating states. In the on-state of the MRC the switches S_1, S_2, S_3 are turned on and S_4, S_5, S_6 are turned off. In the off-state of the MRC the switches S_4, S_5, S_6 are turned on and S_1, S_2, S_3 are turned off. Schematic diagrams for both operating states are shown in Fig. 5.

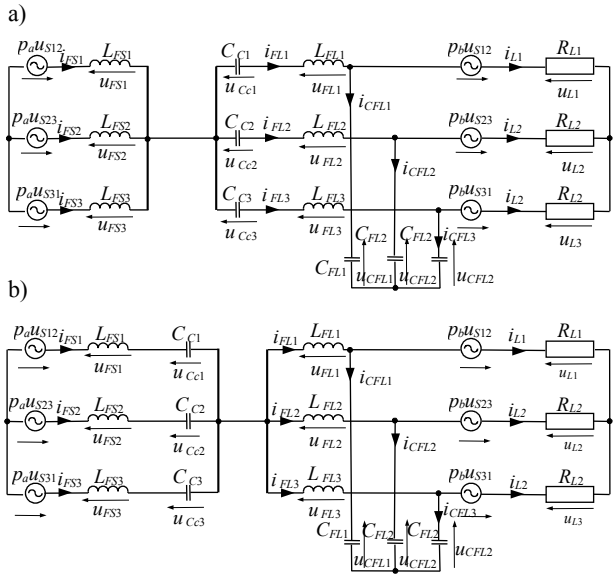

Fig.5. Schematic diagrams of the presented HT, a) for on-state, b) for off-state

For the schematic diagram shown in Fig. 4, the averaged state-space equation can be written as:

$$\begin{aligned} \dot{\overline{\mathbf{x}}} &= \mathbf{A}(D)\overline{\mathbf{x}} + \mathbf{B}(D)u_S \\ \overline{\mathbf{y}} &= \mathbf{C}(D)\overline{\mathbf{x}} + \mathbf{D}(D)u_S \end{aligned}, \tag{6}$$

where $\overline{\mathbf{x}} = \begin{bmatrix} i_{FS} & u_{Cc} & i_{FL} & u_{CFL} \end{bmatrix}^T$ - vector of the averaged variables, $\mathbf{A}(D)$ – averaged state matrix, $\mathbf{B}(D)$ – averaged input matrix, $\mathbf{C}(D)$ – averaged output matrix, $\mathbf{D}(D)$ – averaged input-output matrix. Assumed symmetrical circuit, $L_{FS1}=L_{FS2}=L_{FS3}=L_{FS}$, $C_{C1}=C_{C2}=C_{C3}=C_C$, $L_{FL1}=L_{FL2}=L_{FL3}=L_{FL}$, $C_{FL1}=C_{FL2}=C_{FL3}=C_{FL}$, averaged matrixes can by written as:

$$\mathbf{A}(D) = \begin{bmatrix} 0 & \dfrac{-(1-D)}{L_{FS}} & 0 & 0 \\ \dfrac{1-D}{C_C} & 0 & \dfrac{D}{C_C} & 0 \\ 0 & \dfrac{-D}{L_{FL}} & 0 & \dfrac{-1}{L_{FL}} \\ 0 & 0 & \dfrac{1}{C_{FL}} & \dfrac{-1}{R_L C_{FL}} \end{bmatrix}, \tag{7}$$

$$\mathbf{B}(D) = \begin{bmatrix} \dfrac{p_a}{L_{FS}} \\ 0 \\ 0 \\ \dfrac{-p_b}{R_L C_{FL}} \end{bmatrix}, \tag{8}$$

$$\overline{y} = \overline{u}_L,\ \mathbf{C}(D) = \mathbf{C} = \begin{bmatrix} 0 & 0 & 0 & 1 \end{bmatrix},\ \mathbf{D}(D) = \mathbf{D} = \begin{bmatrix} p_a \end{bmatrix}. \tag{9}$$

From equations, (6) – (9) we can easily obtain the three-phase averaged circuit model (Fig. 6).

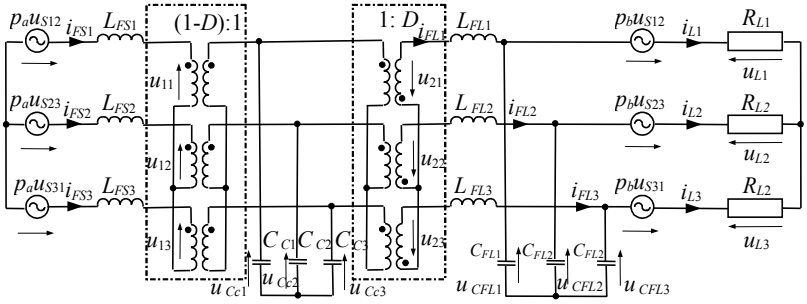

Fig.6 Averaged circuit model of the considered HT

3.2 D-Q transformation of the averaged model of HT

For analysis, the three-phase averaged circuit model (Fig. 6) is transferred to d-q coordinate system. The d-q transformation is defined as [23]:

$$\mathbf{x}_{qd0} = \mathbf{K}\mathbf{x}_{abc}\,,\ \mathbf{x}_{abc} = \mathbf{K}^{-1}\mathbf{x}_{qd0}\,, \tag{10}$$

where

$$\mathbf{K} = \sqrt{\frac{2}{3}}\begin{bmatrix} \cos(\omega t) & \cos\left(\omega t - \frac{2\pi}{3}\right) & \cos\left(\omega t + \frac{2}{3}\pi\right) \\ \sin(\omega t) & \sin\left(\omega t - \frac{2\pi}{3}\right) & \sin\left(\omega t + \frac{2\pi}{3}\right) \\ \frac{1}{\sqrt{2}} & \frac{1}{\sqrt{2}} & \frac{1}{\sqrt{2}} \end{bmatrix}, \tag{11}$$

$$\mathbf{x}_{abc} = \begin{bmatrix} x_a \\ x_b \\ x_c \end{bmatrix},\ \mathbf{x}_{qd0} = \begin{bmatrix} x_q \\ x_d \\ x_0 \end{bmatrix}, \tag{12}$$

where x_q – forward (rotating) phasor, x_d – backward (rotating) phasor, x_0 – zero-sequence component.

The phase source voltages with angular speed ω are assumed ideal and symmetrical and are described by (13).

$$\mathbf{u}_s = \begin{bmatrix} u_{S1} \\ u_{S2} \\ u_{S3} \end{bmatrix} = U_S\sqrt{\frac{2}{3}}\begin{bmatrix} \sin(\omega t + \varphi_1) \\ \sin(\omega t - \frac{2\pi}{3} + \varphi_1) \\ \sin(\omega t + \frac{2\pi}{3} + \varphi_1) \end{bmatrix} \tag{13}$$

Secondary voltages of TR take into account transformer voltage ratio p_a and p_b, and are described by (14) and (15) respectively.

$$p_a\mathbf{u}_s = p_aU_S\sqrt{\frac{2}{3}}\begin{bmatrix}\sin(\omega t+\varphi_1)\\ \sin(\omega t-\frac{2\pi}{3}+\varphi_1)\\ \sin(\omega t+\frac{2\pi}{3}+\varphi_1)\end{bmatrix}, (14) \quad p_b\mathbf{u}_s = p_bU_S\sqrt{\frac{2}{3}}\begin{bmatrix}\sin(\omega t+\varphi_1)\\ \sin(\omega t-\frac{2\pi}{3}+\varphi_1)\\ \sin(\omega t+\frac{2\pi}{3}+\varphi_1)\end{bmatrix}. (15)$$

The d-q transformation of the secondary voltages of TR (Fig. 4) is described as (16) and (17) [24].

$$p_a\mathbf{u}_{Sqd0} = p_a\mathbf{u}_S\mathbf{K} = p_aU_S\begin{bmatrix}\sin\varphi_1\\ \cos\varphi_1\\ 0\end{bmatrix}, (16) \quad p_b\mathbf{u}_{Sqd0} = p_b\mathbf{u}_S\mathbf{K} = p_bU_S\begin{bmatrix}\sin\varphi_1\\ \cos\varphi_1\\ 0\end{bmatrix}, (17)$$

where φ_1 is an initial angle of voltage phase shift.

The equations (18) – (21) described the d-q transformation of three-phase inductor set L_{FS} of the MRC.

$$L\dot{\mathbf{i}}_{LFS} = \mathbf{u}_{LFS}, \tag{18}$$

Substituting $\mathbf{i}_{LFS}$ (19), and according to (10) and taking the derivative (18) becomes (20)

$$\mathbf{i}_{LFS} = I_{LFS}\sqrt{\frac{2}{3}}\begin{bmatrix}\sin(\omega t+\varphi_2)\\ \sin(\omega t-\frac{2\pi}{3}+\varphi_2)\\ \sin(\omega t+\frac{2\pi}{3}+\varphi_2)\end{bmatrix} \tag{19}$$

where φ_2 is the initial angel of the current phase shift.

$$L\left[\left(\dot{\mathbf{K}}^{-1}\right)\mathbf{i}_{LFSqd0} + \mathbf{K}^{-1}\dot{\mathbf{i}}_{LFSqd0}\right] = u_{LFS}. \tag{20}$$

Arranging and solving equation (16) we obtain:

$$L\dot{\mathbf{i}}_{LFSqd0} = -L\mathbf{K}\left(\dot{\mathbf{K}}^{-1}\right)\mathbf{i}_{LFSqd0} + \mathbf{K}\mathbf{u}_{LFS} = -L\omega\begin{bmatrix}0 & 1 & 0\\ -1 & 0 & 0\\ 0 & 0 & 0\end{bmatrix}\mathbf{i}_{LFSqd0} + \mathbf{u}_{LFSqd0} \tag{21}$$

By the same method, the three-phase output inductor set L_{FL} of the MRC is transformed to a d-q coordinate system. Schematic diagrams of inductances L_{FS} and L_{FL} before and after d-q transformation are shown in Figs. 7c and 7d [24].

The equations (22) – (23) describe the d-q transformation of capacitances C_C of the MRC.

$$C_C\dot{\mathbf{u}}_{Cc} = \mathbf{i}_{Cc}. \tag{22}$$

Considering $\mathbf{u}_{Cc}$ in accordance with (10) and taking the derivative (22), we obtain (23).

$$C_C\left[\left(\dot{\mathbf{K}}^{-1}\right)\mathbf{u}_{Ccqd0} + \mathbf{K}^{-1}\dot{\mathbf{u}}_{Ccqd0}\right] = \mathbf{i}_{Ccqd0}\,. \tag{23}$$

Solving equation (23) we obtain:

$$C_C\dot{\mathbf{u}}_{Ccqd0} = -C_C\mathbf{K}\left(\dot{\mathbf{K}}^{-1}\right)u_{Ccqd0} + \mathbf{K}\mathbf{i}_{Cc} = -C\omega\begin{bmatrix}0 & 1 & 0\\ -1 & 0 & 0\\ 0 & 0 & 0\end{bmatrix}\mathbf{u}_{Cc} + i_{Ccqd0} \tag{24}$$

By the same method, three-phase output capacitor set C_{LF} of MRC is transformed to a d-q coordinate system. Schematic diagrams of capacitances C_C and C_{FL} before and after d-q transformation are shown in Figs. 7e and 7f.

As is visible on Fig. 6 there are two sections of switches, described as an ideal transformer (1-D):1 and 1:D. The d-q transformation of these transformers is described by (24) – (27). Transformation of source switches is written as:

$$\mathbf{u}_{Cc} = \mathbf{u}_1\left(\mathbf{I} - \mathbf{D}\right), \tag{24}$$

The equation (24) is transformed to a d-q coordinate system and then can be described by (25).

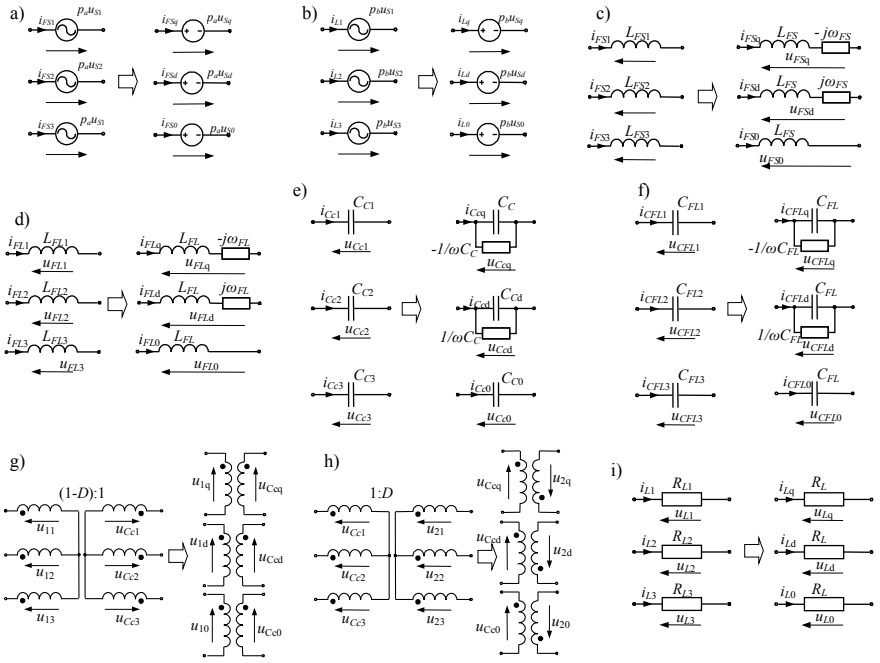

Fig.7. The schematic diagrams before and after d-q transformation, a), b) secondary voltages with transformer voltage ratio p_a *and* p_b *of TR, c) input inductances of the MRC, d) output inductance of the MRC, e) capacitances of the MRC, f) output filter capacitances, g), h) source and load switches of the MRC, i) load resistances*

$$\mathbf{u}_{Ccqd0} = \mathbf{u}_1\mathbf{K}(\mathbf{I} - \mathbf{D}) = u_{1qd0}\begin{bmatrix} 1-D & 0 & 0 \\ 0 & 1-D & 0 \\ 0 & 0 & 1-D \end{bmatrix}. \tag{25}$$

Transformation of load switches is written as:

$$\mathbf{u}_1 = \mathbf{u}_{Cc}\mathbf{D}. \tag{26}$$

The equation (26) is transformed to a d-q coordinate system and then can be described by (27)

$$\mathbf{u}_{1qd0} = \mathbf{u}_{Cc}\mathbf{K}\mathbf{D} = u_{Ccqd0}\begin{bmatrix} D & 0 & 0 \\ 0 & D & 0 \\ 0 & 0 & D \end{bmatrix}. \tag{27}$$

Schematic diagrams before and after a d-q transformation of the switches of the MRC are shown in Figs. 7g and 7h.

The d-q transformation of load resistance is described as:

$$\mathbf{u}_{Lqd0} = \mathbf{K}\mathbf{u}_L = \mathbf{K}R_L\mathbf{i}_{Lqd0} = R_L\mathbf{i}_{Lqd0}. \tag{28}$$

Schematic diagrams before and after a d-q transformation of load resistance is shown in Fig. 7i.

The steady state characteristic can be obtained by considering the single-phase d-q transformed circuit of the presented HT. The d-q transformed schematic diagrams of the considered HT for backward and forward component are shown in Fig. 15.

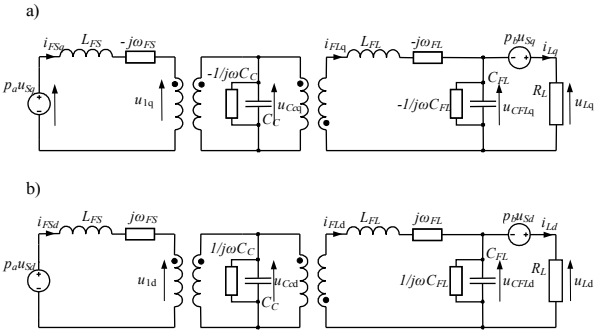

Fig.15 The d-q transformed circuit of HT, a) for forward component, b) for backward component.

Assuming a symmetrical and balanced circuit of the HT and conditions described by (29) we obtain a circuit only for forward (rotating) phasor component (30).

$$\varphi_1 = 0. \tag{29}$$

According to (10) and taking into account (29), d-q transformed source voltages are described as:

$$\mathbf{u}_{Sqd0} = U_S \begin{bmatrix} 0 \\ 1 \\ 0 \end{bmatrix}. \tag{30}$$

According to (30) a d-q transformed schematic diagram of the presented HT for steady state analysis (DC model) is divided into four terminal networks and is shown in Fig. 16.

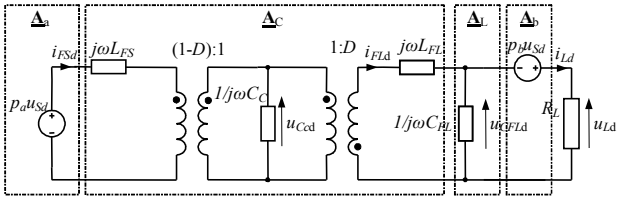

Fig.16. DC model of considered HT: $\underline{\boldsymbol{A}}_a$ – chain matrix of the secondary windings a, $\underline{\boldsymbol{A}}_b$ – chain matrix of the secondary windings b, $\underline{\boldsymbol{A}}_C$ – chain matrix of the MRC basic structure, $\underline{\boldsymbol{A}}_L$ – chain matrix of the HT output filter

Taking into account p_a and p_b such as voltage transformer ratio secondary windings *a* and *b* respectively (Fig.1), the four-terminal chain equations are described as (31) – (34).

$$\underline{\mathbf{A}}_a = \begin{bmatrix} \dfrac{1}{p_a} & 0 \\ 0 & p_a \end{bmatrix}, \qquad (31)\ \underline{\mathbf{A}}_b = \begin{bmatrix} \dfrac{1}{p_b} & 0 \\ 0 & p_b \end{bmatrix}, \tag{32}$$

$$\underline{\mathbf{A}}_L = \begin{bmatrix} 1 & 0 \\ j\omega C_L & 1 \end{bmatrix}, \tag{33}$$

$$\underline{\mathbf{A}}_C = \begin{bmatrix} \dfrac{(1-D)^2 - \omega^2 L_S C}{D(1-D)} & \dfrac{j\omega\left[(1-D)^2 L_L - L_S\left(\omega^2 L_L C - D^2\right)\right]}{D(1-D)} \\ \dfrac{j\omega C}{D(1-D)} & \dfrac{\omega^2 L_L C - D^2}{D(1-D)} \end{bmatrix}. \tag{34}$$

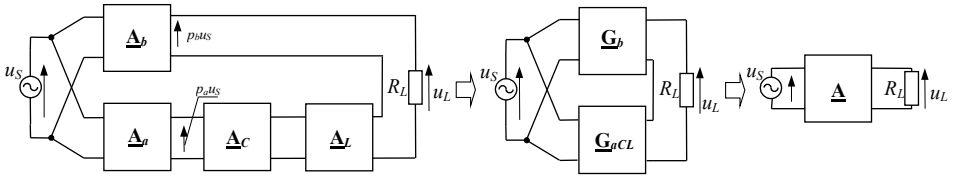

Fig.17. Substitute diagram four-terminal networks connections of the considered HT

$$\begin{bmatrix} \underline{U}_S \\ \underline{I}_S \end{bmatrix} = \underline{\mathbf{A}} \begin{bmatrix} \underline{U}_L \\ \underline{I}_L \end{bmatrix} = \begin{bmatrix} \underline{A}_{11} & \underline{A}_{12} \\ \underline{A}_{21} & \underline{A}_{22} \end{bmatrix} \begin{bmatrix} \underline{U}_L \\ \underline{I}_L \end{bmatrix} = \frac{1}{\underline{G}_{21}} \begin{bmatrix} 1 & -\underline{G}_{22} \\ \underline{G}_{11} & -\det \underline{\mathbf{G}} \end{bmatrix} \begin{bmatrix} \underline{U}_S \\ \underline{I}_L \end{bmatrix}, \tag{35}$$

where $\underline{\mathbf{G}} = \underline{\mathbf{G}}_a + \underline{\mathbf{G}}_{aCL}$.
The parameters of the $\underline{\mathbf{G}}_b$ and $\underline{\mathbf{G}}_{aCL}$, there are four-terminal hybrid parameters, which are shown in the appendix in table I and II. In accordance with four terminal theories, we obtain:

$$\underline{H}_U = \frac{\underline{U}_L}{\underline{U}_S} = \frac{1}{\underline{A}_{11} + \underline{A}_{12}/R_L}, \tag{36}$$

$$\arg \underline{H}_U = \arg\left(\frac{1}{\underline{A}_{11} + \underline{A}_{12}/R_L} \right) \tag{37}$$

$$\lambda_S = \frac{P_S}{S_S} = \cos\left[\arg\left(\frac{\underline{A}_{11}R_L + \underline{A}_{12}}{\underline{A}_{21}R_L + \underline{A}_{22}} \right) \right] \tag{38}$$

The characteristics of magnitude and phase of the voltage transmittance and input power factor obtained by means of (36) – (38) for circuit parameters collected in the Tab. III are shown in section four. For purpose of comparison, these characteristics are presented together with ones obtained by means of simulation investigations of the presented circuit with idealized switches (Fig. 4).

3.3 Small signal model of HT

It is assumed that all variables have two components: a running constant component (the averaged value in the switching period T_S), which is marked by upper case letter, and perturbation marked by lower case letter, straddled by the symbol "^".

$$\begin{aligned} &i_{FS} = I_{FS} + \hat{i}_{FS}, u_{Cc} = U_{Cc} + \hat{u}_{Cc}, i_{FL} = I_{FL} + \hat{i}_{FL} \\ &u_{CL} = U_{CL} + \hat{u}_{CL}, d = D + \hat{d} \end{aligned} \tag{39}$$

On the basis of the averaged state space method the small signal state space equations are expressed as [22]:

$$\frac{d}{dt}(\mathbf{X} + \hat{\mathbf{x}}) \approx \mathbf{A}\hat{\mathbf{x}} + \mathbf{B}\hat{\mathbf{u}} + [(\mathbf{A}_1 - \mathbf{A}_2)\mathbf{X} + (\mathbf{B}_1 - \mathbf{B}_2)\mathbf{U}]\hat{d}, \tag{40}$$

where $\mathbf{A}_1 = \mathbf{A}(D)$ for $D = 0$, $\mathbf{A}_2 = \mathbf{A}(D)$ for $D = 1$. According to (35), the Laplace transform for small signal state-space equation is expressed as (41) and (42):

$$s\hat{\mathbf{x}}(s) = \mathbf{A}\hat{\mathbf{x}}(s) + \mathbf{B}\hat{\mathbf{u}}(s) + [(\mathbf{A}_1 - \mathbf{A}_2)\mathbf{X} + (\mathbf{B}_1 - \mathbf{B}_2)\mathbf{U}]\hat{d}(s), \tag{41}$$

$$\hat{u}_L(s) = \mathbf{C}\hat{\mathbf{x}}(s) + \mathbf{D}\hat{\mathbf{u}}(s). \tag{42}$$

Solving equations (36) and (37) we obtain:

$$\begin{aligned} &\hat{\mathbf{x}}(s) = (s\mathbf{I} - \mathbf{A})^{-1}\left\{\mathbf{B}\hat{\mathbf{u}}(s) + [(\mathbf{A}_1 - \mathbf{A}_2)\mathbf{X} + (\mathbf{B}_1 - \mathbf{B}_2)\mathbf{U}]\hat{d}(s)\right\} = \\ &= \mathbf{G}_{\hat{\mathbf{x}},\hat{\mathbf{u}}}(s)\mathbf{u}(s) + \mathbf{G}_{\hat{\mathbf{x}},\hat{d}}(s)\hat{d}(s) \end{aligned} \tag{43}$$

$$\hat{u}_L(s) = \left[\mathbf{C}\mathbf{G}_{\hat{\mathbf{x}},\hat{\mathbf{u}}}(s) + \mathbf{D}\right]\hat{\mathbf{u}}(s) + \left[\mathbf{C}\mathbf{G}_{\hat{\mathbf{x}},\hat{d}}(s)\right]\hat{d}(s) = \\ = \mathbf{G}_{\hat{u}_L,\hat{\mathbf{u}}}(s)\hat{\mathbf{u}}(s) + \mathbf{G}_{\hat{u}_L,\hat{d}}(s)\hat{d}(s) \quad , \tag{44}$$

where:

$$\mathbf{G}_{\hat{\mathbf{x}},\hat{\mathbf{u}}} = \frac{\hat{\mathbf{x}}(s)}{\hat{\mathbf{u}}(s)}, \tag{45}$$

$$\mathbf{G}_{\hat{\mathbf{x}},\hat{d}} = \frac{\hat{\mathbf{x}}(s)}{\hat{d}(s)}, \tag{46}$$

$$\mathbf{G}_{\hat{u}_L,\hat{\mathbf{u}}} = \frac{\hat{u}_L(s)}{\hat{\mathbf{u}}(s)}, \tag{47}$$

$$\mathbf{G}_{\hat{u}_L,\hat{d}} = \frac{\hat{u}_L(s)}{\hat{d}(s)}. \tag{48}$$

The dependencies (45) – (48) are shown in the appendix in table IV. The calculation and simulation test results of the transient states of the considered HT are shown in the next section.

4 SIMULATION TEST RESULTS

The parameters of the investigated circuit (Fig. 1) are the same as the ones in the theoretical analysis and are given in the appendix in table III. The presented results have been obtained for load matching conditions described by (59).

$$\sqrt{\frac{L_{FS}}{C_C}} = \sqrt{\frac{L_{FL}}{C_{FL}}} = R_L . \tag{59}$$

Exemplary simulation time waveforms of load voltage u_L of the presented HT, for different value of pulse duty factor D, are shown in Fig. 18.

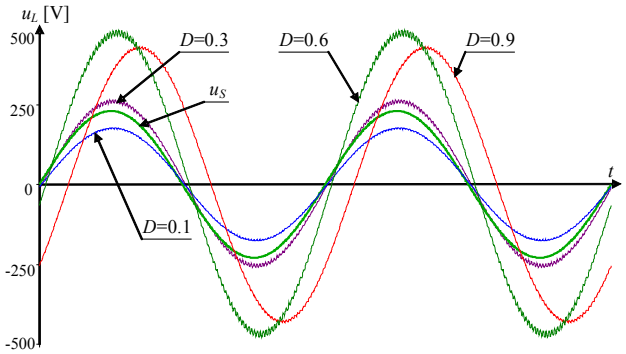

Fig.18. Exemplary simulation time waveforms of load voltage of presented HT for different value D

The characteristics of magnitude (36) and phase of voltage transmittance (37), as a function of duty pulse factor D, are shown in Figs. 19a and 19b respectively. Characteristic of input power factor as a function of duty pulse factor D is shown in Fig. 19c.

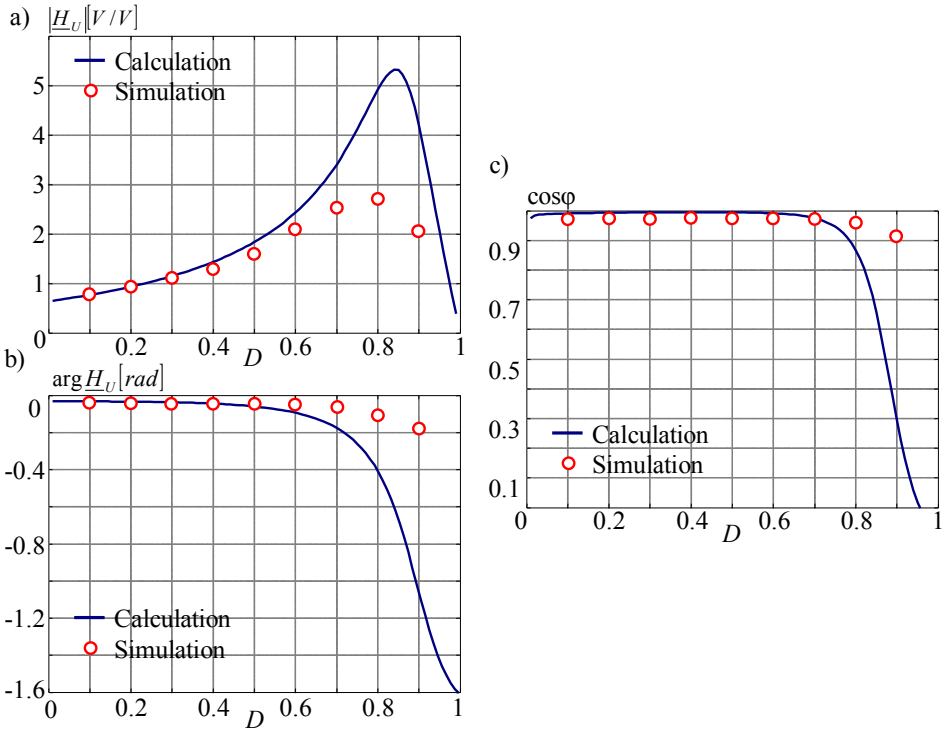

Fig.19 Static characteristics of a) magnitude b) phase of voltage transmittance c) input power factor of the presented HT as a function D

As is visible in Figs 18 and 19a, the output voltage of the presented HT (u_L) is dependent on the value of duty pulse factor D. The output voltage u_L is less or approximately equal to the source voltage u_S for $D \leq 0.2$. The output voltage is greater than the source voltage for $D > 0.2$. In the considered HT the range of change of the output voltage u_L is from $0.66u_S$ to more than $2.5u_S$ (Figs 18 and 19a).The phase shift between source voltage u_S and load voltage u_L occurring for the value of duty factor D is because of resonance phenomena in MRC circuit [21].

The calculation and simulation test results of transient states of considered HT at 50 % step-up and 50 % step-down of supply voltage u_S with duty factor $D = 0.25$ is shown in Figs. 21 and 22 respectively.

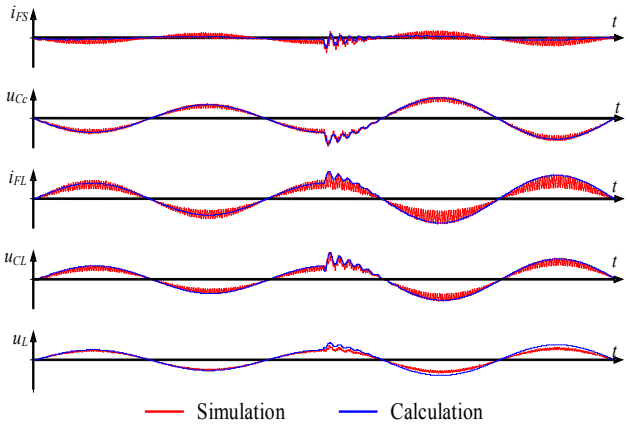

Fig.21 Transient states of HT at 50% step-up of supply voltage where D = 0.25

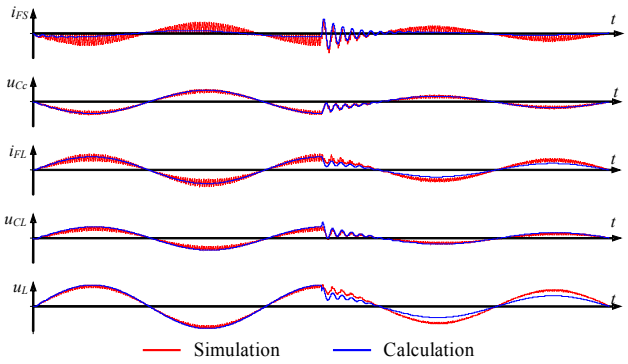

Fig.22. Transient states of HT at 50% step-down of supply voltage where D = 0.25

A is visible from Figs 21 and 22, calculation and simulation test results converge.

5 CONCLUSIONS

In this paper a new solution for a three-phase hybrid transformer using matrix-reactance chopper with Ćuk topology has been presented. The proposed solution of HT satisfies both favourable effective number of switches and voltage transforming properties. In the presented HT the possibility of obtaining the range of change of the load voltage from 0.66 to more then 2.5 of source voltage has been shown. The nominal output voltage can be obtained even at 50% step-down or step-up of the source voltage. The simulation test results have confirmed the results of theoretical results. Further research will be focused on construct experimental model to verify both simulation and calculation results, and to decrease oscillation during step-up and step-down of supply voltage.

6 APPENDIX

Table I

G_{b11}	0
G_{b12}	$1/p_b$
G_{b21}	p_b
G_{b22}	0

Table II

G_{aCL11}	$\frac{jp_a^2\omega\left(C - C_L D^2 + CC_L L_L \omega^2\right)}{\left(-1+D\right)^2 + \left(-CL_s + C_L j^2\left(\left(-1+D\right)^2 L_L + D^2 L_s\right)\omega^2 - CC_L j^2 L_L L_s \omega^4\right)}$
G_{aCL12}	$\frac{p_a\left(\left(-1+D\right)^2 D^2 + C\left(-1+j^2\right)\left(\left(-1+D\right)^2 L_L + D^2 L_s\right)\omega^2 - C^2\left(-1+j^2\right)L_L L_s \omega^4\right)}{\left(-1+D\right)D\left(\left(-1+D\right)^2 + \left(-CL_s + C_L j^2\left(\left(-1+D\right)^2 L_L + D^2 L_s\right)\omega^2 - CC_L j^2 L_L L_s \omega^4\right)\right)}$
G_{aCL21}	$\frac{\left(-1+D\right)Dp_a}{\left(-1+D\right)^2 + \left(-CL_s + C_L j^2\left(\left(-1+D\right)^2 L_L + D^2 L_s\right)\omega^2 - CC_L j^2 L_L L_s \omega^4\right)}$
G_{aCL22}	$-\frac{j\omega\left(D^2 L_s + L_L\left(\left(-1+D\right)^2 - CL_s\omega^2\right)\right)}{\left(-1+D\right)^2 + \left(-CL_s + C_L j^2\left(\left(-1+D\right)^2 L_L + D^2 L_s\right)\omega^2 - CC_L j^2 L_L L_s \omega^4\right)}$

Table III

symbol	value
u_S	3 x 400 V / 50 Hz
p_a	4/3
p_b	2/3
L_S	1 mH
C	10 µF
L_L	1 mH
C_L	10 µF
Z_L	10 Ω
f_S	5 kHz

Table IV

$G_{\hat{i}_{FS},\hat{u}}$	$\frac{s^3 C_C C_L L_{FL} R_L p_a + s^2 C_C L_{FL} p_a + s\left(C_C p_a R_L + D^2 C_L p_a R_L\right) + \left(-1+D\right)Dp_b}{M}$
$G_{\hat{u}_{Cc},\hat{u}}$	$\frac{s^2\left(1-D\right)C_L L_{FL} p_a R_L + s\left(\left(1-D\right)L_{FL} p_a + DL_{FS} p_b\right) - \left(-1+D\right)p_a R_L}{M}$
$G_{\hat{i}_{FL},\hat{u}}$	$\frac{s^2 C_C L_{FS} p_b + s\left(-1+D\right)DC_L p_a R_L + \left(-1+D\right)Dp_a + \left(-1+D\right)^2 p_b}{M}$
$G_{\hat{u}_{CL},\hat{u}}$	$\frac{-s^3 C_C L_{FL} L_{FS} p_b + s\left(-\left(-1+D\right)^2 L_{FL} p_b - D^2 L_{FS} p_b\right) + \left(-1+D\right)Dp_a R_L}{M}$
$G_{\hat{u}_L,\hat{u}}$	$\frac{s^4 C_C C_L L_{FS} L_{FL} p_b R_L + s^2\left(\left(-1+D\right)^2 C_L L_{FL} p_b R_L + \left(C_C + D^2 C_L\right)L_{FS} p_b R_L\right)}{M} + \frac{\left(-1+D\right)Dp_a R_L + \left(-1+D\right)^2 p_b R_L}{M}$
M	$s^4 C_C C_L L_{FL} L_{FS} R_L + s^3 C_C L_{FL} L_{FS} + s^2\left(\left(-1+D\right)^2 C_L L_{FL} R_L + \left(C_C + D^2 C_L\right)L_{FS} R_L\right) + s\left(\left(-1+D\right)^2 L_{FL} + D^2 L_{FS}\right) + \left(-1+D\right)^2 R_L$

7 REFERENCE

[1] EN 50160, *Voltage characteristics of electricity supplied by public distribution systems*.

[2] Conrad. L, Little K., Grigg C.: *Predicting and preventing problems associated with remote fault – clearing voltage dips*, IEEE Trans. Ind. Applications, vol. 27, No.1, pp. 167-172 , 1991.

[3] Milanowić J., Hiskansen I.: *Effect of load dynamics on power system damping*, IEEE Trans. on Power System Vol. 10 No. 2, pp. 1022 -1028 May 1995.

[4] Bollen M., Zang L.: *Analysis of voltage tolerance of ac adjustable – speed drives for three phase balanced and unbalanced sags*, IEEE Trans. on Ind. Applic., vol. 36 No.3, pp. 904 - 910 May / June 2000

[5] Duran-Gomez J., Prased P., Enjeti N., Woo B.: *Effect of voltage sags on adjustable-speed drives: a critical evaluation on an approch to improve performance*, IEEE Trans. on Ind. Application, vol. 35, No. 6, pp. 1440 - 1449 Nov./Dec. 1999.

[6] Falce A., Matas G., Da Silva Y.: *Voltage sag analysis and solution for an industrial plant with embedded induction motors*, in Proc. 2004 Ind. Applications Conference 2004, vol. 4 pp.2573 – 2578 Oct.

[7] Montero-Hernandez O., Enjeti P.: *Application of a boost ac-ac converter to compensate for voltage sags in electric power distribution system*, in Proc. 2000 IEEE 31TH Power Engineering Society Transmission and Distribution Conf. pp. 470 – 475.

[8] Oliviera J., Freitas L., Viera J. Jr.: *A serial regulator using soft switching PWM ac/ac full bridge converter*, in Proc. 1999 IEEE 30TH Power Engineering Society Transmission and Distribution Conf. pp. 193 – 198.

[9] Oliviera J., Freitas L., Coelho E., Farias V., Viera J. Jr.: *A PWM ac/ac full bridge used like a shunt and a serial regulator*, in Proc. 1997 European Conference on Power Electronics and Applications. Trondheim. pp. 2.186-2.191.

[10] Jang D., Choe G.: *Step-up/down ac voltage regulator using transformer with tap changer and PWM ac chopper*, IEEE Trans. on Ind. Electronics, vol. 45 No. 6 pp. 905 - 911 December 1998.

[11] Fedyczak Z., Frąckowiak L., Jankowski M, Kempski A.: *Single – phase serial ac voltage controller based on bipolar PWM ac matrix – reactance chopper*, in Proc. 2005 11TH European Conference on Power Electronics and Applications, Dresden.

[12] Harada K., Anan F., Yamasaki K., Jinno M., Kawata Y., Nakashima T., Murata K, Sakamoto H.: *Inteligent transformer*, PESC'96 Italy vol.2 pp. 1337 - 1341 Baveno June 1996.

[13] Aeloiza E., Enjeti P., Moran L., Pite I.: *Next generation distribution transformer: to address power quality for critical loads*, PESC'03 IEEE vol. 3 pp.1266 – 1271 June 2003.

[14] Aeloiza E., Prased P., Enjeti P., Moran L., Montero-Hernandez O., Kim S.: *Analysis and design of new voltage sag compensator for critical loads in electric power distribution system*, IEEE Trans. on Ind. Applications, vol. 39 No.4, pp.1143 - 1150 July / Aug. 2003.

[15] Lee D., Habetler T., Harley R., Rostron J., Keister T.: *A voltage sag supporter utilizing a PWM-switched autotransformer*, IEEE Power Elect. Spec. Conf., PESC'04, Aachen, 2004 pp. 4244 – 4250.

[16] Yorino N., Danyoshi M., Kitagawa M.: *Interaction among multiple controls in tap change under load transformers*, IEEE Trans. on Power System, vol. 12, No. 1. pp.: 430-436, 1997.

[17] Kaniewski J.: *Single phase hybrid transformer using matrix converter*, Wiadomości Elektrotechniczne 03.2006, pp: 46-48. (In Polish)

[18] Fedyczak Z., Kaniewski J.: *Single phase hybrid transformer using matrix-reactance chopper with Ćuk topology*, in Proc. 12th European Conference on Power Electronics and Applications, Aalborg 2007

[19] Fedyczak Z., Kaniewski J.: *Single phase hybrid transformer using bipolar matrix – reactance chopper*, Przegląd Elektrotechniczny, 07-08.2006, pp: 80-85. (In Polish)

[20] Fedyczak Z., Kaniewski J.: *Modelin and analysis of three-phase hybrid transformer using matrix converter*, *in Proc. 5th International Conference-Workshop – CPE 2007*, 29 May – 01 June, Gdańsk

[21] Fedyczak Z.: *PWM AC voltage transforming circuits*, University of Zielona Góra Press, Zielona Góra 2003. (In Polish)

[22] Middlebrook R. D., Ćuk S.: *A general unified approach to modelling switching-converter power stages*, PESC'76 Conf. Rec. pp.18–34, 1976.

[23] Choi N., Li Y.: *Modelling and Analysis of AC Line Conditioner Based on Three-Phase PWM Ćuk AC-AC Converter*, in Proc. 2004 The 30th Annual Conf. of the IEEE Ind. Electr. Society, 2-6 Nov, Busan, Korea.

[24] Chen J., Ngo K. D. T.: *Graphical Phasor Analysis of Three-Phase PWM Converters*, IEEE Trans. on Power Electronics, vol. 16, NO. 5, September 2001